Sedimentary Geology 442 (2022) 106278

Contents lists available at ScienceDirect

Sedimentary Geology

journal homepage: www.elsevier.com/locate/sedgeo

Detrital zircon U–Pb ages and trace elements indicate the provenance of Early Carboniferous Li-rich claystone from central Guizhou, South China

Jihua Yang [a,c,d], Hanjie Wen [b,d,*], Xinzhuan Guo [c], Chongguang Luo [a], Wenxiu Yu [e], Shengjiang Du [f], Yi Cui [g], Bo Zhao [h]

[a] State Key Laboratory of Ore Deposit Geochemistry, Institute of Geochemistry, Chinese Academy of Sciences, Guiyang 550081, China
[b] School of Earth Sciences and Resources, Chang'An University, Xi'an 710054, China
[c] CAS Key Laboratory of High-temperature and High-pressure Study of the Earth's Interior, Institute of Geochemistry, Chinese Academy of Sciences, Guiyang 550081, China
[d] College of Earth and Planetary Sciences, University of Chinese Academy of Sciences, Beijing 100049, China
[e] Faculty of Land Resource Engineering, Kunming University of Science and Technology, Kunming 650093, China
[f] School of Mining Engineering, Guizhou Institute of Technology, Guiyang 550003, China
[g] State Key Laboratory of Nuclear Resources and Environment, East China University of Technology, Nanchang 330013, China
[a] Shaanxi Provincial Land Engineering Construction Group Co., Ltd., Shaanxi Xi'an 710075, China

ARTICLE INFO

Article history:
Received 6 May 2022
Received in revised form 20 October 2022
Accepted 21 October 2022
Available online 27 October 2022

Editor: Dr. Brian Jones

Keywords:
Jiujialu Formation
Lithium
Clay
Detrital zircon
Provenance
Early Palaeozoic intracontinental orogeny

ABSTRACT

Lithium is of great importance for green energy technology, and most industrial Li is sourced from brine lakes and pegmatites. Recently, strong Li enrichment has been reported in the late Palaeozoic Jiujialu Formation (C_1jj) in Guizhou, South China; however, the source and the sedimentary processes that formed the Jiujialu Formation remain unclear. We present the U–Pb ages and trace element compositions of detrital zircon grains from the Jiujialu Formation and underlying dolomite of the Loushanguan Group ($Cam_{2-3}ls$), which indicate the grains in the Jiujialu Formation on the margin of the Central Guizhou Uplift and in a depression in southeast Guizhou have three primary age peaks (1000–900, ~760, and ~530 Ma). These ages are similar to those of Ordovician strata, indicating a contribution from the Ordovician strata to the Jiujialu Formation in these areas. Detrital zircon grains from the Jiujialu Formation in the core of the Central Guizhou Uplift and the Loushanguan Group have two primary age peaks at ~760 and ~530 Ma, which suggests that the underlying Loushanguan Group supplied most of the material to the Jiujialu Formation in this area. The age distribution of detrital zircon grains indicates that sediment erosion from the sedimentary stratal transport was limited, and deposition occurred near the direct source. In addition, the trace element compositions of the detrital zircon grains indicate that their original source was magmatic rocks of the South China Block. An early Palaeozoic intracontinental orogeny in South China uplifted subduction-related magmatic rocks (1000–900 Ma) in the northeast of the South China Block, exposing them to weathering and providing material for the Ordovician strata. This suggests that the weathering of sedimentary strata can form clay-type Li deposits in areas with carbonate bedrock, and that the provenance of Cambrian–Ordovician sedimentary strata in the Yangtze Block was controlled by an early Palaeozoic intracontinental orogeny.

1. Introduction

Lithium is classified as a critical element by many countries due to the increasing demand for Li-ion batteries, which have a high power density and relatively low cost, making them ideal for energy storage in portable electronic devices, electrical power grids, and the growing fleet of hybrid and electric vehicles (Tarascon, 2010; Benson et al., 2017). Traditional types of Li ore include Li pegmatites, brine deposits, and Li-rich volcanism-related clay ores (Kesler et al., 2012), which account for 64 %, 29 %, and 7 % of global Li ore resources, respectively (Paul et al., 2011). Recently, a new type of Li-rich claystone deposit related to carbonate weathering has been reported in late Palaeozoic strata of central Guizhou and central Yunnan, China, and this discovery has important implications for Li resource exploration and could enhance the supply of Li resources (Wen et al., 2020). The provenance of this new Li-rich claystone deposit is important to understand the difference between this and other types of Li deposits, especially volcanism-related Li-rich claystone ores, and to improve the understanding of Li mineralization. The Li-rich claystone of the Jiujialu Formation in central Guizhou is found mostly over a single area of carbonate bedrock (details in Section 2.3) and is an ideal area to study the provenance of this type of Li-rich claystone. Many previous studies have suggested that the

* Corresponding author at: School of Earth Sciences and Resources, Chang'An University, Xi'an 710054, China.
E-mail address: wenhanjie@vip.gyig.ac.cn (H. Wen).

https://doi.org/10.1016/j.sedgeo.2022.106278
0037-0738/

underlying dolomite was the main provenance of the Li-rich claystone, based on rare earth element (REE) patterns, immobile element (e.g., Zr, Hf, Nb, Ta) ratios, and geological observations (Hu et al., 1988; Gao et al., 1992; Wen et al., 2020); however, this hypothesis is still debated because of the complex effects of lateritic weathering (Gu et al., 2013). Many studies have shown that some heavy minerals are resistant to intense weathering, are not affected by laterization, and can be used to trace the source of sediments (Gu et al., 2013; Zhang et al., 2020). Zircon is the most frequently used of these resistant minerals due to its widespread occurrence in magmatic, metamorphic, and sedimentary rocks. Zircon is physically and chemically stable, and is resistant to alteration by geological processes such as weathering, transportation, and erosion (Siebel et al., 2009). Consequently, the oldest crust on Earth contains intact zircon grains (with ages of ~4.4 Ga) despite the effects of many geological events through time (Mojzsis et al., 2001; Nemchin et al., 2006). In addition, the trace element composition of zircon is controlled by its crystallisation environment; hence, we can determine the tectonic setting in which a zircon crystallised by analysing its trace element composition (Belousova et al., 2002). On this basis, many studies have analysed the trace element composition and chronology of multiple recycling cycles of detrital zircon grains from sedimentary rocks and ores to trace their ultimate and/or direct sources, sedimentary processes, and tectonic evolution (Gu et al., 2013; Hou et al., 2017; Wang et al., 2018; Zhao and Liu, 2019; Zhu et al., 2020; Zhang et al., 2021; Xiong et al., 2021).

The Jiujialu Formation is widely distributed around Xiuwen, Jinsha, and a depression to the southeast that includes the areas of Kaili, Huangping, and Majiang. We report the U–Pb ages and trace element compositions of detrital zircon grains from the underlying dolomite of the Loushanguan Group ($Cam_{2-3}ls$) and Li-rich claystone of the Jiujialu Formation in the three areas. We also consider previously published data. Combining these data with the history of continental collision and orogenesis in South China, we find that the provenance of the Jiujialu Formation is bedrock, and confirm that clay-type Li deposits can form from erosion from proximal carbonate bedrock. This is a different origin than volcanic-related Li-rich claystone. The magmatic rocks of the South China Block were the ultimate source of the zircons. Variations in the provenance of Cambrian–Ordovician sedimentary strata in the Yangtze Block were controlled by an early Palaeozoic intracontinental orogeny, and raise a new insight on the early Palaeozoic provenance variation of the Yangtze Block.

2. Geological setting

2.1. Regional geology

The South China Block consists of the Yangtze Block in the northwest and the Cathaysia Block in the southeast, separated by the Jiangnan Orogenic Belt (Fig. 1A, B). The Yangtze and Cathaysia blocks have Archean–Palaeoproterozoic basement, including the Kongling complex (2900–2400 Ma) in the north of the Yangtze Block (Gao et al., 1999; Qiu et al., 2000) and the Badu Group (2000–1800 Ma) to the southwest of Zhejiang in the Cathaysia Block (Zhao and Cawood, 1999). The basement records the growth of Archean crust in South China. In addition, many zircon grains inherited from Archean volcanic rocks have been found in lamprophyre dykes in Jingshan (Hubei province), Ningxiang (Hunan province), and Zhenyuan (Guizhou province) with ages of mainly 2900–2500 Ma, indicating that the Archean basement represented by the Kongling complex is distributed widely across the Yangtze Block (Zheng et al., 2006).

The Proterozoic evolution of the South China Block was closely related to the assembly and fragmentation of Rodinia (Geng et al., 2020). During the early Neoproterozoic (1000–900 Ma), the ancient South China Ocean plate was subducted beneath the southeast margin of the Yangtze Block (Fig. 1C), producing arc magmatic rocks in the northeastern part of the South China Block (e.g., the Shuangxiwu arc 1000–900 Ma; Fig. 1B; Li et al., 2008a, 2009; Shu, 2012). The Cathaysia and Yangtze blocks collided at ~830 Ma, forming the Jiangnan Orogenic Belt (e.g., the Sibao and Fanjiangshan groups; Zheng and Zhang, 2007). During the middle–late Neoproterozoic, the northwestern margin of the Yangtze Block was an extensional or rifting setting (Fig. 1C). The Neoproterozoic (835–720 Ma) igneous rocks on the western and northwestern margins of the Yangtze Block are mainly mafic dyke swarms and bimodal volcanic rocks (e.g., the Suxiong Group; 806–803 Ma; Li et al., 2001; X.L. Wang et al., 2012). Rifting peaked at 790–760 Ma (Li et al., 2008a, 2008b). The Jiangnan Orogenic Belt in central China underwent extensional collapse, resulting in post-collisional magmatism (Zheng and Zhang, 2007). The major rifting event lasted until the middle–late Neoproterozoic, and a minor rifting event is recorded in the southwestern part of the Yangtze Block lasted until Cambrian, including a volcanic metamorphic porphyry or tuff in the Meishucun Formation that yields zircon U–Pb ages of 539.4 ± 2.9 Ma (Compston et al., 2008) and 535.2 ± 1.7 Ma (Zhu et al., 2009).

During the early Palaeozoic, the southeastern part of South China experienced a strong compressional intracontinental orogeny, and granites and mafic rocks were emplaced at 460–400 Ma across the Cathaysia Block and the Jiangnan Orogenic Belt (Fig. 1B; Faure et al., 2009). Most of these igneous rocks are granitoids, with minor mafic rocks in the Wuyi–Nanling–Yunkai region (Fig. 1B; Zhang et al., 2012; Kong et al., 2020). The present study area is located within the Yangtze Block, in Guizhou Province, southwestern China (Fig. 1B).

2.2. Palaeogeography

During the middle Cambrian, the Yangtze Block began to amalgamate with Gondwana; however, no large-scale orogeny occurred, and carbonate platform deposits remained relatively stable (Wen, 2013). The Kangdian landmass formed high topography in the northwest (Fig. 2A). Low-lying marine deposits formed in the southeast (Wen, 2013). During the late Cambrian, the assembly of Gondwana was complete, and the palaeogeographic pattern was similar to that of the middle Cambrian (Fig. 2B). Emergent land, clastic tidal flats, carbonate platforms, continental slope, and a marine basin setting developed successively from west to east (Fig. 2B; Wen, 2013).

Central Guizhou was not uplifted above sea level during the Cambrian–Early Ordovician. During the early Palaeozoic, the southeastern part of South China experienced a strong compressional intracontinental orogeny (Faure et al., 2009), and a large-scale marine regression occurred during the Wufengian (late Ordovician, equivalent to Ashgillian), enlarging the Kangdian landmass. Uplift related to this orogeny also formed the Central Guizhou landmass (Fig. 2C; Feng et al., 2004). Southeast Guizhou was lower than central Guizhou due to an east–west syncline to the south of the central Guizhou anticline and movement on the Guiyang Huangping Fault Zone (Fig. 3C; Niu et al., 2007). During the Longmaxi and Shiniulanian (early Silurian, equivalent to Llandovery), the crust subsided after the Duyun Orogeny, and marine sedimentation occurred in southeastern Guizhou (Niu et al., 2007). By the end of the Silurian, southeastern Guizhou was uplifted again during the Caledonian Orogeny.

The upper Yangtze landmass drifted to the warm, wet climate of the low-latitude Intertropical Convergence Zone during the Late Palaeozoic (Yu et al., 2019). Intense weathering and erosion resulting in the absence of Devonian, Silurian, and some Ordovician strata in central Guizhou (Fig. 3B; Deng et al., 2010), levelled the uplifted area and formed a quasi-karst plain, which included karst depressions and basins into which the Jiujialu Formation clay and bauxite were deposited during the early Carboniferous (Gao et al., 1992).

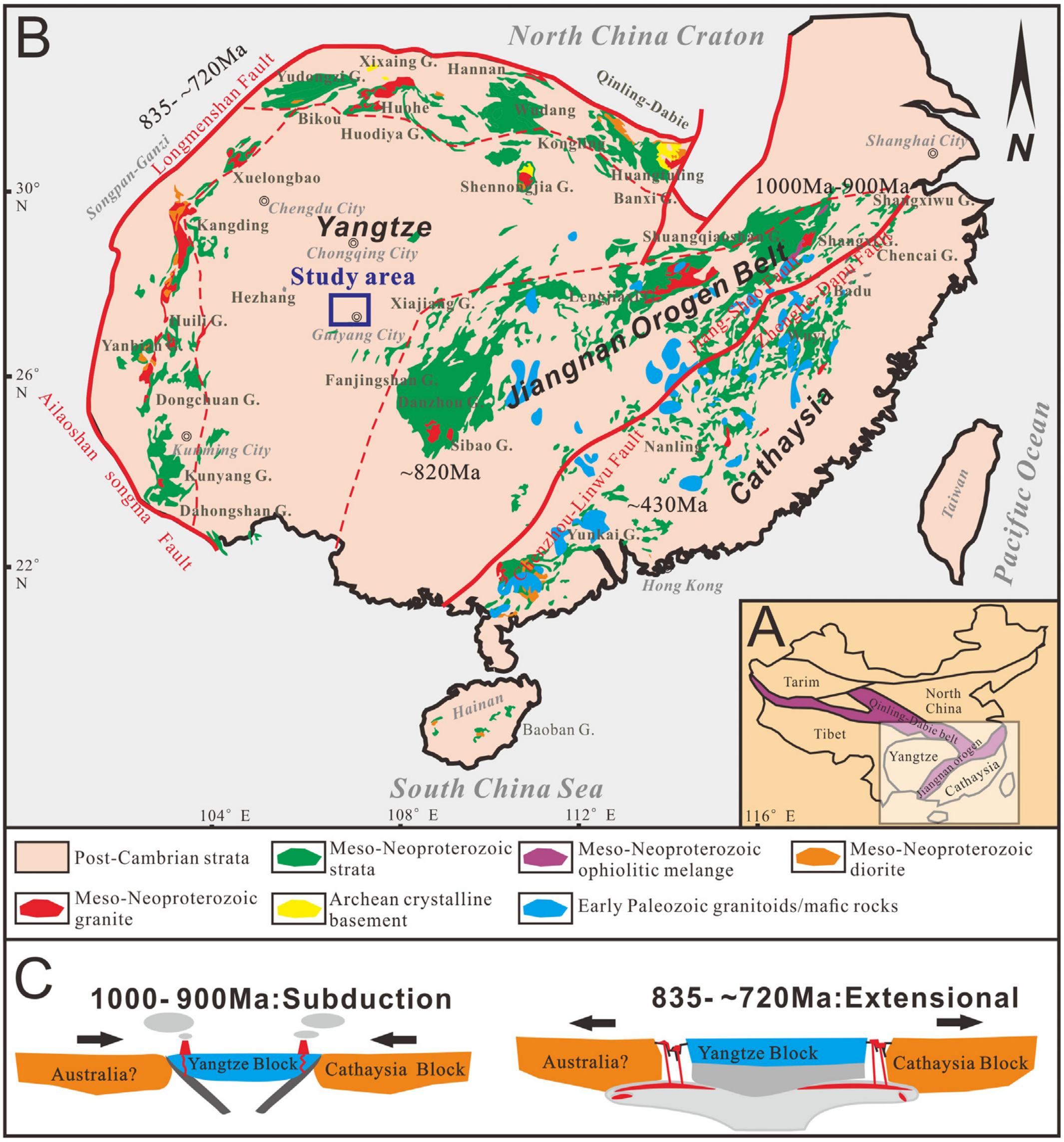

Fig. 1. (A) Outline and position of the South China Block. (B) Distribution and ages of Mesoproterozoic–Neoproterozoic and early Palaeozoic magmatic rocks and strata in the South China Block (modified after Xu and Du, 2018; Geng et al., 2020). (C) Evolution of South China Block during Late Mesoproterozoic to Middle Neoproterozoic (modified after Li et al., 2008a).

2.3. Geological features

The Jiujialu Formation is typically composed of three units with a total thickness of 5–20 m. The upper unit consists of coal interbedded with clay and black carbonaceous shale, the middle unit comprises clay and bauxite layers, and the lower unit comprises iron-rich layers that are composed primarily of ferruginous clay and limonite (Fig. 4). The Jiujialu Formation distribution and thickness were controlled by the palaeokarst topography. The strata that underlie the Jiujialu Formation change from the core to the margin of the Central Guizhou anticline, and include dolomite of the lower Cambrian Qingxudong (Cam$_1$q) and middle Cambrian Gaotai (Cam$_2$g) and Shilengshui (Cam$_2$s) Formations; dolomite of the middle–upper Cambrian Loushanguan Group (Cam$_{2-3}$ls); and dolomite, mudstone, shale, and carbonaceous mudstone of the Lower Ordovician Tongzi (O$_1$t), Honghuayuan (O$_1$h), and Meitan (O$_1$m) Formations (Figs. 3B, 4). The Loushanguan Group dolomite is the most widely distributed unit underlying the Jiujialu Formation (Gao et al., 1992). Three representative sections of Li-rich claystone in southeast Guizhou were similar to that in central Guizhou (Fig. 4), but it was uplifted later than central Guizhou and experienced a greater number of transgression–regression cycles. The basement in Southeast Guizhou includes dolomite of the middle–upper Cambrian Loushanguan Group (Cam$_{2-3}$ls) and Lower Ordovician Tongzi (O$_1$t) and Upper Devonian Gaopochang (D$_3$gp) Formations (Figs. 3B, 4C).

3. Sampling and analytical methods

3.1. Sampling

3.1.1. Li-rich rocks of the Jiujialu Formation

In central Guizhou, two aggregate Li-rich claystone samples were collected from two typical sections of the Jiujialu Formation in the Jinsha area (GDDY-1 and GDDY-2). The two sections are ~4 km apart and the Li content in each section is ~400–1000 ppm (Fig. 3B, C). Southeast of Guizhou, three aggregate Li-rich claystone samples were collected from the Jiujialu Formation at Majiang (MJJ), Yudong (LCYD), and Huangping (HPC). The mean Li contents in the three sections are ~300–600 ppm, and the three samples were taken 15–20 km apart (Fig. 3B, C). The Li-rich claystone was sampled by collecting 5–8 typical ore samples over ~20 m along the strike of the seam, with a total weight of 7–10 kg. Small pieces of uniform size with a total weight of 2–3 kg were selected from each sample for zircon separation.

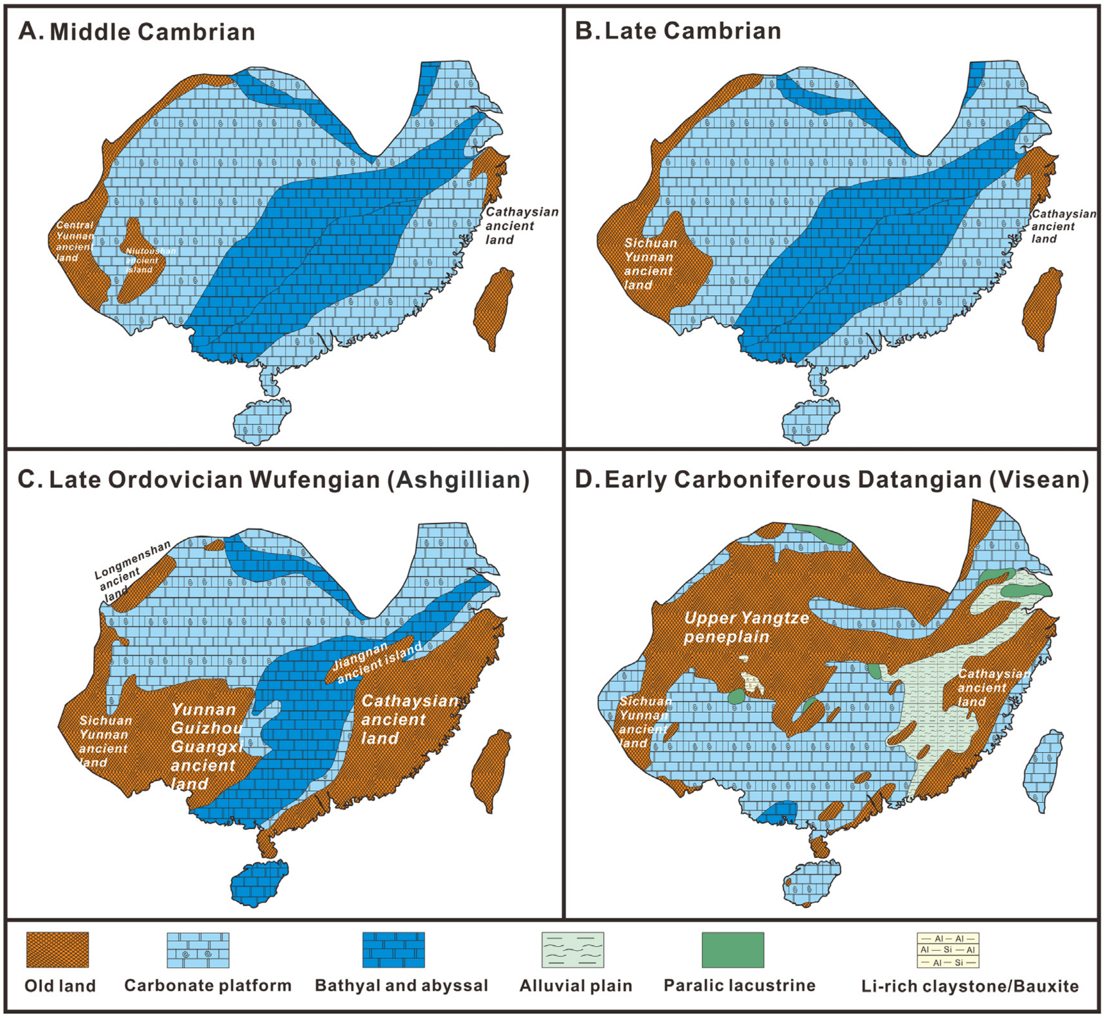

Fig. 2. Palaeogeography of the South China Block during (A) the middle Cambrian, (B) the late Cambrian, (C) the Wufengian (late Ordovician, equivalent to Ashgillian), and (D) the Datangian (early Carboniferous, equivalent to Visean).
(Modified after Liu and Xu (1994).)

3.1.2. Dolomite of the Loushanguan Group

Two aggregate dolomite samples from the Loushanguan Group were collected ~3 km apart in the Jinsha area (LSG-1 and LSG-2) in central Guizhou (Fig. 3B, C). The dolomite sampling involved collecting ~30 dolomite samples with a total weight of ~10 kg over ~100 m along the strike of the bed. Half of each sample, with a total weight of ~5 kg, was selected for zircon separation. The samples were crushed, dissolved in concentrated HCl, and stirred slowly to remove as much of the carbonate minerals as possible. After dissolution was complete (3–4 days), the remaining sediment and incompletely dissolved dolomite fragments were extracted and dried for zircon separation.

3.1.3. Detrital zircon separation

Zircon separation was conducted at Wuhan Sample Solution Analytical Technology (Wuhan, China). The collected samples were crushed and ground. Then, heavy minerals were separated from light minerals by elutriation. The mineral groups that contained zircon were then placed on an Al plate for magnetic separation. Finally, the zircon grains were sorted under a binocular microscope. The purity of the sorted zircon grains was ≥99 %.

3.2. In situ LA–ICP–MS zircon U–Pb dating and trace element analyses

U–Pb ages and trace element compositions of the zircon grains were measured using a laser ablation–inductively coupled plasma–mass spectrometer (LA–ICP–MS) at Wuhan Sample Solution Analytical Technology (Wuhan, China). The detailed analytical conditions were the same as those described by Hu et al. (2015) and Zong et al. (2017). An Excel-based program (ICPMSDataCal) was used to perform off-line data selection, background integration, signal analysis, time drift corrections, and quantitative calibration for the trace element analyses and U–Pb dating (Liu et al., 2008; Liu et al., 2010). Concordia diagrams and weighted mean calculations were carried out using Isoplot/Ex version 3 (Ludwig, 2003). We excluded ages with concordance of <90 % and used $^{206}Pb/^{238}U$ ages for grains younger than 1000 Ma and $^{207}Pb/^{206}Pb$ ages for older grains. A total of 284 zircon grains from GDDY-1 and GDDY-2; 350 zircon grains from MJJ, LCYD and HPC; and 126 zircon grains from LSG-1 and LSG-2 were analysed.

3.3. Classification and regression tree scheme

The trace element composition of zircon is affected by the crystallisation environment, as shown by correlations between the trace element patterns of zircon grains and the composition of the host magma. Belousova et al. (2002) analysed the trace element compositions of many zircon grains from different rock types and proposed the classification and regression tree (CART) scheme (Fig. 5) for distinguishing the parent rock type of individual zircon grains. We used the CART method to define the parent rock type of the zircon grains, and we

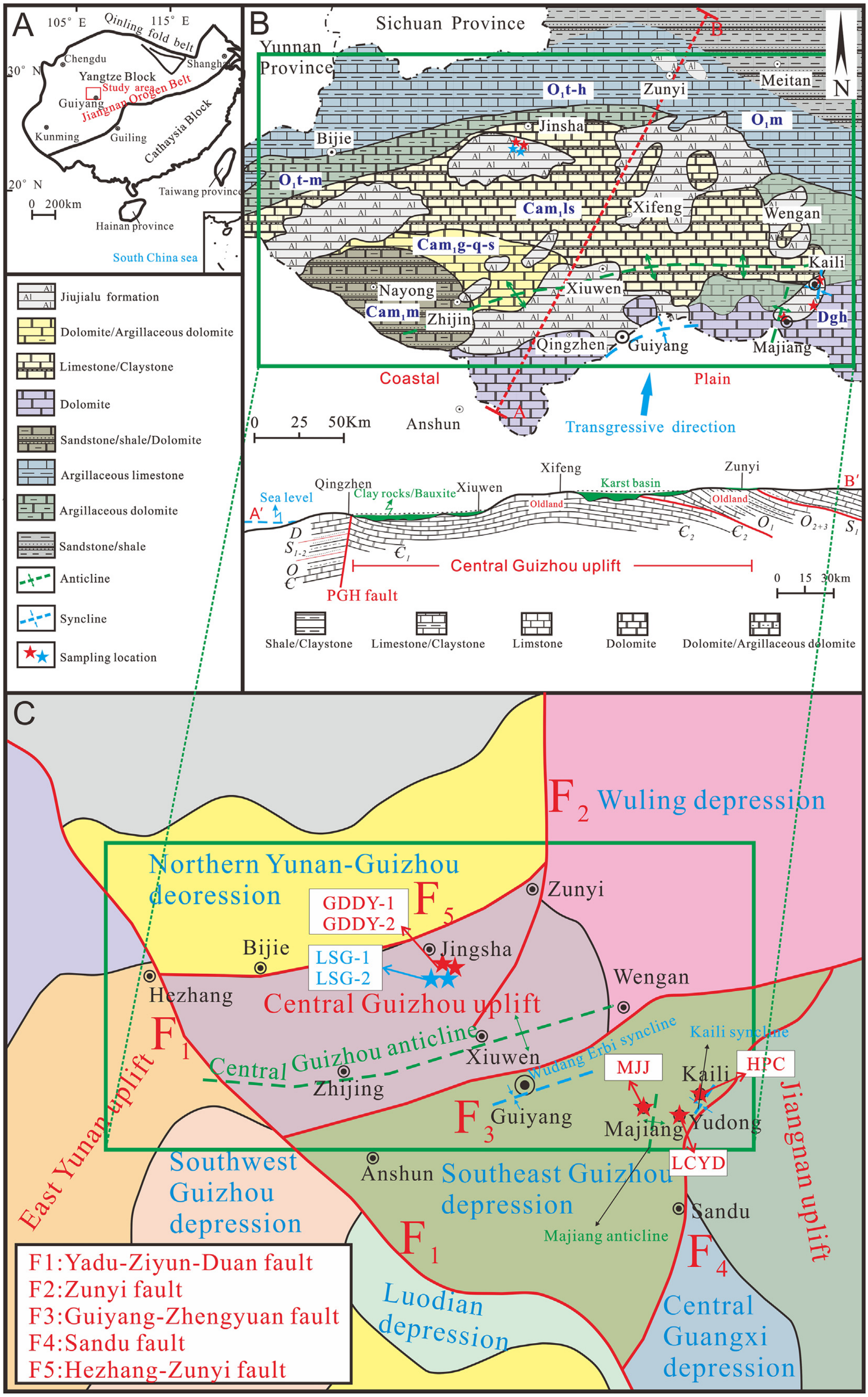

Fig. 3. (A) Tectonic framework of China showing the location of the South China Block. (B) Simplified geological map of the Li-rich claystone deposits in the study area (modified after Gao et al., 1992; Ling et al., 2020). (C) Structural map of the Central Guizhou Uplift and the Yunnan Guangxi region (modified after Niu et al., 2007; Deng et al., 2010).

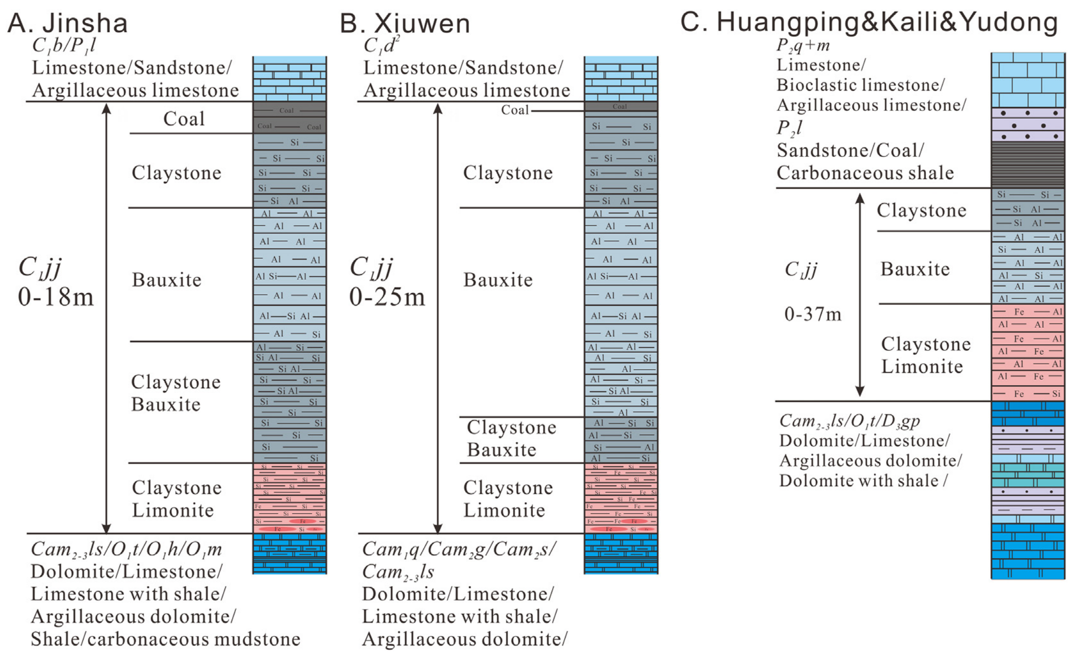

Fig. 4. Stratigraphic column of the study area.

combine the CART results from individual zircon grains with their U–Pb ages to recreate the tectonic evolution and to determine the source of the Li-rich claystone.

4. Results

4.1. Zircon cathodoluminescence images and trace element compositions

4.1.1. Cathodoluminescence images

Cathodoluminescence (CL) images of detrital zircons reveal the morphology, zoning, and integrity of the crystals, which record the genesis of the parent rock and transportation of the zircon grains (Gu et al., 2013; Zhao and Liu, 2019). The CL images of selected detrital zircon grains from this study are show in Fig. 6. Most grains have clear oscillatory zoning that is indicative of a magmatic origin, whereas others have weak oscillatory zoning, suggesting a mafic magmatic or metamorphic origin. Most grains are broken and rounded, suggesting a distal source or multiple recycling cycles or deposition–weathering–transport.

4.1.2. Th/U ratios

Zircon grains from samples GDDY-1 and GDDY-2 have Th/U ratios of 0.01–5.73. A total of 91.2 % of the zircon grains have Th/U ratios of >0.2. Zircon grains from samples MJJ, LCYD and HPC have Th/U ratios of 0.02–3.6. In addition, 93.7 % of these zircon grains have Th/U ratios of >0.2. Zircon grains from LSG-1 and LSG-2 have Th/U ratios of 0.14–2.07. A total of 95.2 % of the zircon grains from these samples have Th/U ratios of >0.2 (Table 1). Th/U ratios suggest most of the zircon grains derived from igneous rocks, and a small part is metamorphic origin.

4.1.3. Classification and regression tree analysis

The trace element compositions of zircon grains can be used to classify the host rocks of zircon grains. We used the CART method to determine the zircon grains' source rocks. The results indicate that most grains were derived from granitoids and mafic rocks (Table 1; Fig. 7). Zircons' age and parent lithology are consistent with each evolution

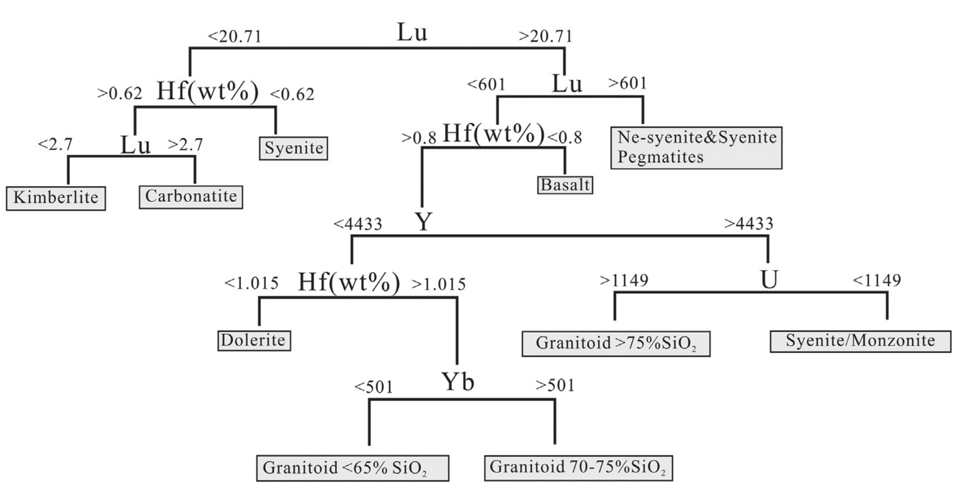

Fig. 5. Classification and regression tree (CART) that distinguishes between zircon grains from different rock types as Belousova et al. (2002) suggested.

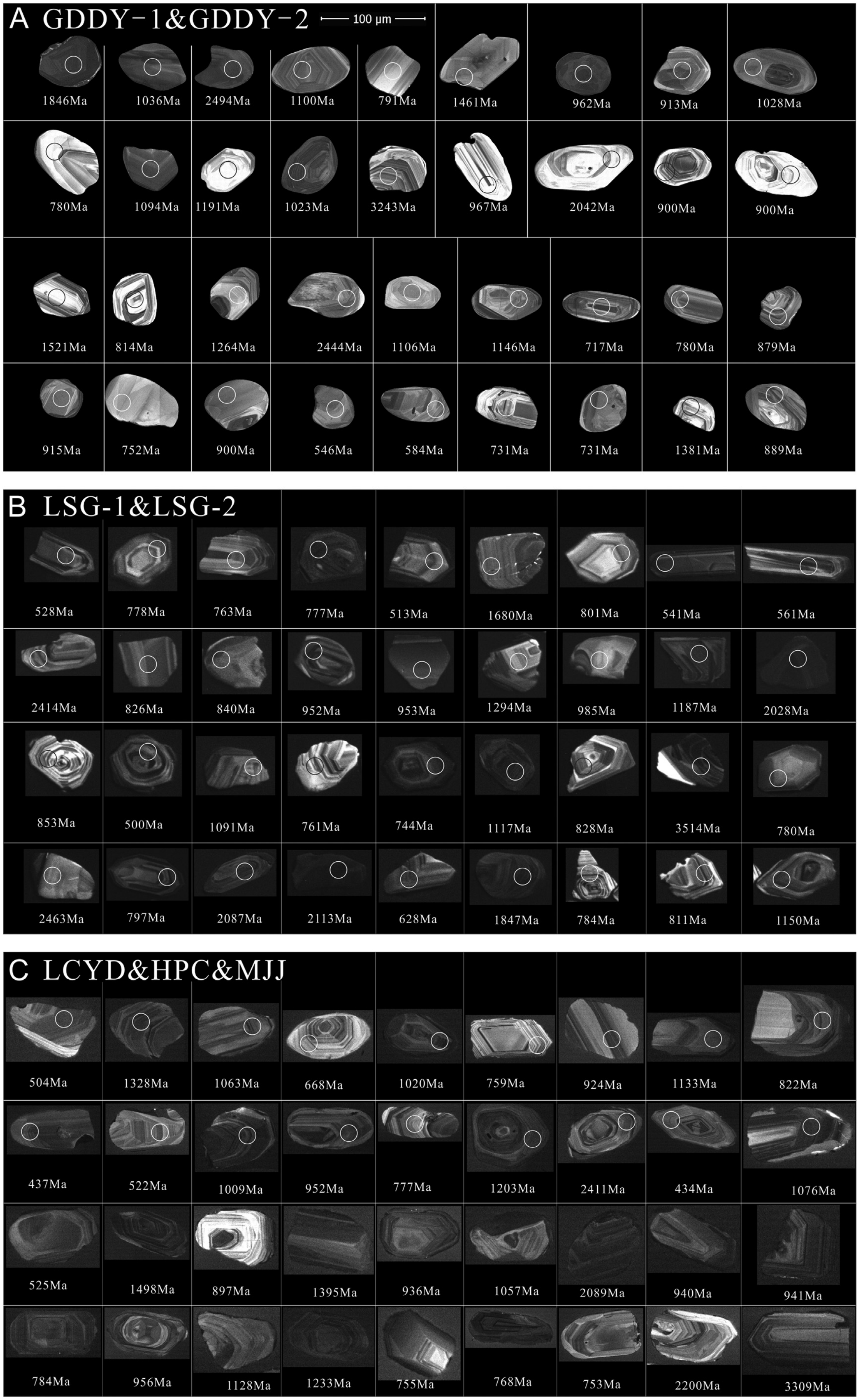

Fig. 6. Representative cathodoluminescence images of zircon grains showing analysis locations and U–Pb ages.

stage of South China Block (Figs. 1C, 12), suggesting multiple sources derived from magmatic rocks around South China Block.

4.2. In situ detrital zircon U–Pb ages

The LA–ICP–MS zircon U–Pb ages are listed in Table 1, concordia diagrams are shown in Fig. 8, and age histograms are shown in Fig. 9. The U–Pb ages of the zircon grains from samples GDDY-1, GDDY-2, MJJ, LCYD and HPC show a similar characteristic and range from ~3800 to ~430 Ma, with large peaks at 1000–900, ~760, and ~530 Ma, and smaller peaks at ~2500, ~650 Ma. The U–Pb ages of the zircon grains from dolomite samples LSG-1 and LSG-2 range from ~3500 to 500 Ma, with large peaks at ~780 and ~530 Ma, and smaller peaks at 650 Ma.

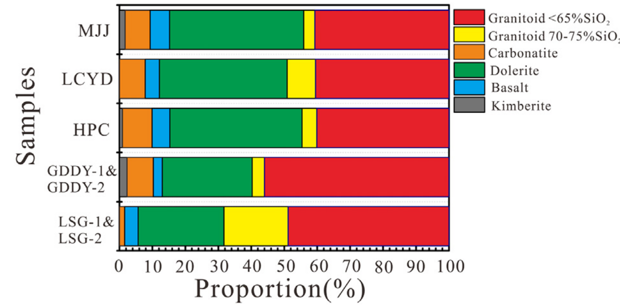

Fig. 7. Results of classification and regression tree (CART) analysis as Belousova et al. (2002) suggested (Table 1), showing the proportion of zircon grains from different rock types in the total detrital zircons; the ordinate displays the sample name.

5. Discussion

5.1. Provenance of the Jiujialu Formation

The sources of sedimentary rocks can be determined by comparing zircon U–Pb ages with the ages of potential provenance areas or units (Fig. 9). Comparison of the probability density plots for the ages of detrital zircon grains in the Jiujialu Formation and Loushanguan Group indicates that the Loushanguan Group is not the only source of zircon crystals in the Jiujialu Formation (Fig. 9A–C, G). Combining our data with detrital zircon ages of the Ordovician Meitan Formation ($O_{1-2}m$) in northeast Guizhou and the Hongshiya Formation ($O_{1-2}h$) in central Yunnan (Fig. 9D, E) suggests that the Ordovician strata in central Guizhou were also a source of material for the Jiujialu Formation.

5.1.1. Loushanguan Group

There is no peak at 1000–900 Ma on a probability density plot of the ages of detrital zircon grains from dolomite of the Loushanguan Group (Fig. 9G), and the detrital zircon grains from the Jiujialu Formation in the Xiuwen area and the Loushanguan Group show similar age peaks (Fig. 9B, G), suggesting that the main source of material in the Xiuwen area was the Loushanguan Group or other Cambrian carbonate units in this area.

5.1.2. Ordovician strata

The Ordovician sedimentary strata show a similar detrital zircon age spectrum to that of the Jiujialu Formation in Jinsha and the southeastern depression (Fig. 9A, C–E), suggesting that the Ordovician strata contributed sediment to the Jiujialu Formation in those areas.

5.1.3. Contribution model

In contrast to the Li-rich claystone in the Jinsha area, the Xiuwen area lacks detrital zircon grains with ages of 1000–900 Ma (Fig. 9B), which reflect the control of the timing of uplift in each part of Central Guizhou on the contribution of material from Ordovician strata. The Xiuwen area was affected by the central Guizhou anticline and was uplifted earlier than the other areas (Deng et al., 2010), resulting in a shorter period of deposition of Ordovician strata and a smaller contribution of these strata to the Jiujialu Formation (Fig. 10). Therefore, the detrital zircon age spectrum of the Li-rich claystone in the Xiuwen area is more similar to that of the Loushanguan Group (Fig. 9B, G). In the Jinsha area and southeastern Guizhou, where uplift occurred later, the Ordovician strata are thicker and there are many sources of weathered material (Fig. 10); hence, the detrital zircon age spectrum of the Li-rich claystone in the Jinsha area and southeastern Guizhou is more similar to that of the Ordovician strata (Figs. 9A, C–E, 10). The detrital zircon grains in the Jiujialu Formation have age peaks controlled by the basement in various locations, which indicates that the transportation of sediment during weathering was limited, and deposition occurred near to the source. The Li-rich claystone of the Jiujialu Formation was recycled from weathered sedimentary strata.

5.2. Provenance of detrital zircon grains and implications for the tectonic evolution

The distribution of the ages of detrital zircon grains from the Li-rich claystone shows four major magmatic events in the region, at ~2500, 1000–900, 790–760 and 644–441 Ma (Fig. 9A–C). These data indicate that significant magmatic events occurred during these periods and provided the primary source of the material in the Jiujialu Formation. Detrital zircon grains with ages of ~2500 Ma are spread throughout the Li-rich claystone deposits in Guizhou. Previous studies have suggested that an important episode of crustal reworking in the Yangtze Block occurred at ~2500 Ma, and these zircon grains are one of most important distinguishing features of the Yangtze Block (Wang et al., 2013), suggesting some of the detrital zircon grains in our samples may have been derived from earlier Palaeoproterozoic rocks in the Yangtze Block.

At 1000–900 Ma the South China Block was affected by subduction-related magmatic activity along its western margin and the Jiangnan Orogenic Belt in the Yangtze Block (Fig. 1C; Li et al., 2002). Subduction-related magmatic rocks are distributed mainly in the northeast of the South China Block (Fig. 1B; Shu, 2012). The zircon grains derived from intermediate-silicic igneous rocks have an age peak at 1000–900 Ma (Fig. 12B). However, in the middle–late Cambrian, both the Jiangnan Orogenic Belt and the Cathaysia Block were in a marine basin (Fig. 11A, B), which would have made it difficult for them to provide material for sedimentary rocks at that time. This may explain the lack of detrital zircon grains with ages of 1000–900 Ma in the Ediacaran and Cambrian strata.

The period after ~835 Ma is characterised by volcanic and intrusive rocks that formed in an extensional setting (Fig. 1C). Bimodal volcanic rocks are distributed along the northwest margin of the Yangtze Block and the Jiangnan Orogenic Belt. The ages of detrital zircon grains derived from mafic and intermediate-silicic igneous rocks show peaks at 790–760 Ma and ~535 Ma (Fig. 12), suggesting regional bimodal magmatic rocks were a source of the zircon grains (Fig. 1C). When the Jiangnan Orogenic Belt was in a marine basin setting, the northwestern part of the South China plate had been uplifted to form a landmass (Fig. 11A, B); therefore, the distribution of detrital zircon ages in the Cambrian strata is similar to that of zircon grains from the period of rifting of the Yangtze Block (Figs. 1C, 9G–I).

During the early Palaeozoic, the southeastern part of South China experienced an intense intracontinental orogeny that uplifted Jiangnan Island and the Cathaysia Block (Fig. 11C), and enhanced the weathering of the subduction-related magmatic rocks that formed in those areas during the late Mesoproterozoic–early Neoproterozoic (1000–900 Ma). This weathering provided many detrital zircon grains with ages of 1000–900 Ma (Fig. 11C), which explains the 1000–900 Ma peak in the ages of detrital zircons from the Ordovician strata. There was also a contribution from early Palaeozoic magmatic rocks (Fig. 11C).

The detrital zircon grains in the Li-rich claystone show a large age peak at 1000–900 Ma (Fig. 9A, C), but this does not mean that

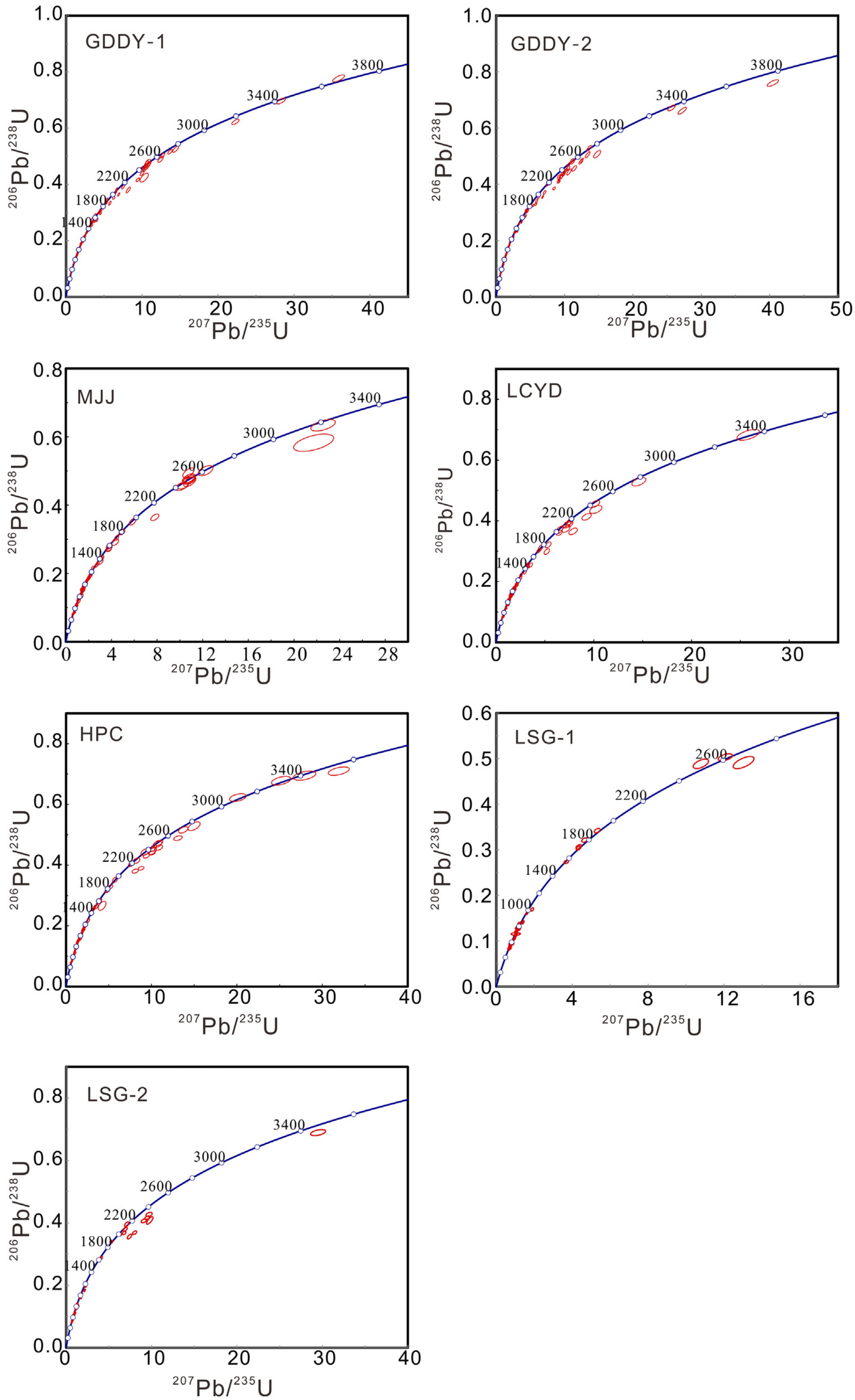

Fig. 8. U–Pb concordia plots for detrital zircon grains.

subduction-related magmatic rocks are the main provenance of the Jiujialu Formation. The zircon fertility of subduction-related magmatic rocks is stronger than that of mafic rocks. Mafic rocks are generally low in zircon but high in clastic material (i.e., feldspar, pyroxene). The mafic rocks on the northwestern margin of Yangtze Block provided clastic material to the sedimentary rocks in Central Guizhou from the Cambrian to the Late Ordovician (Fig. 11A–C). The proportion of zircon grains derived from mafic rocks is 26 %–40 % (Table 1; Fig. 7). Therefore,

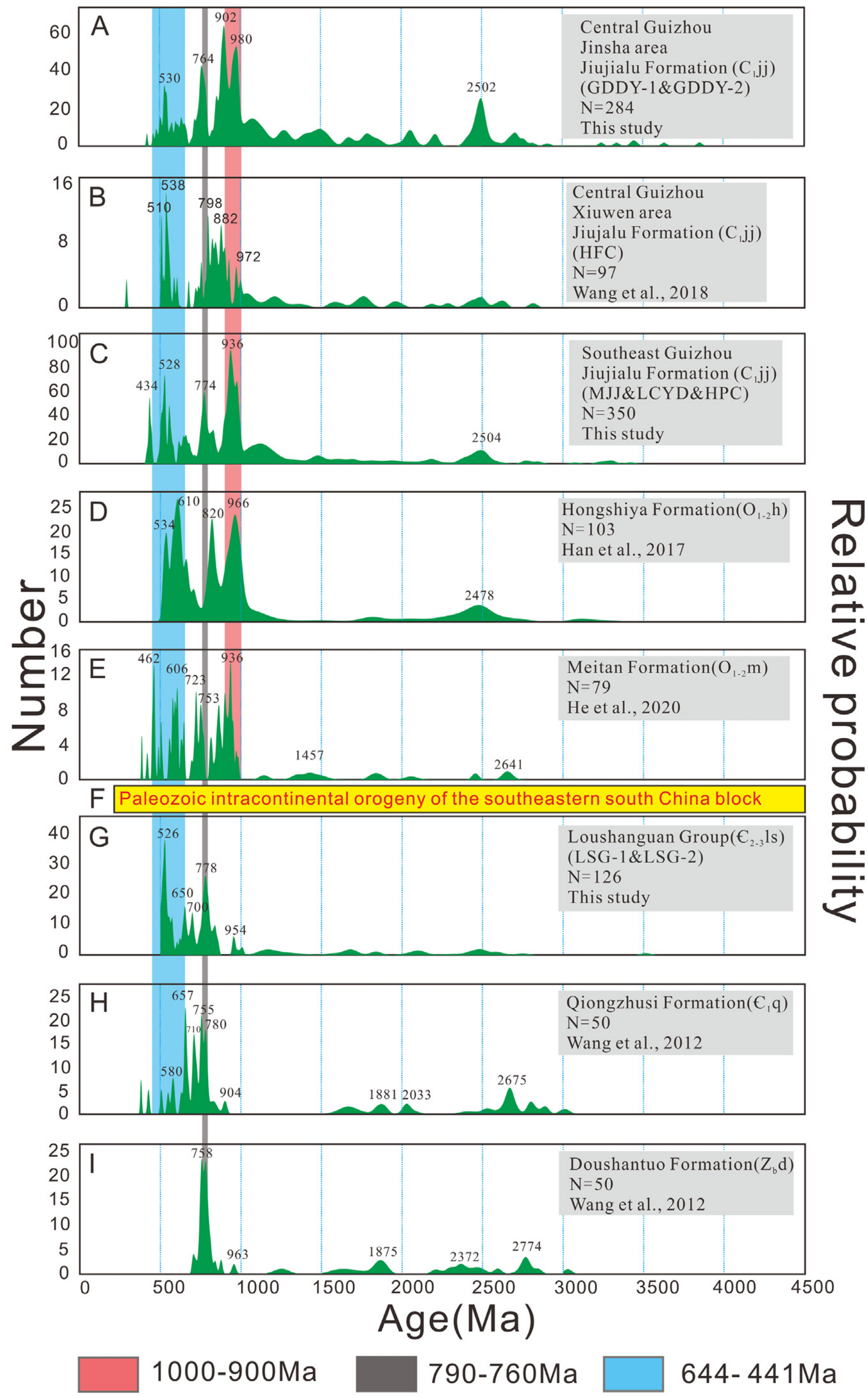

Fig. 9. Age histograms for detrital zircon grains from different strata. Data for the Hongshiya Formation (O$_{1-2}$h) are from Han et al. (2017), for the Meitan Formation (O$_{1-2}$m) from He et al. (2020), for the Qiongzhusi (Cam$_1$q) and Doushantuo (Z$_b$d) formations from L.J. Wang et al. (2012) and for the Jiujialu Formation (C$_1$jj) in the Xiuwen area from Wang et al. (2018).

we suggest that the mafic rocks at the northwest margin of the Yangtze Block were initially the primary source of clastic material in the Jiujialu Formation.

5.3. Formation of Li-rich claystone

From the late Mesoproterozoic to the early Neoproterozoic, subduction-related tectonic activity and rifting events around Yangtze Block formed abundant magmatic rocks, which provide most of the material for the sedimentary strata in central Guizhou. The source area during each period was controlled by palaeogeography. During the Late Ordovician, the central Guizhou area was affected by the Central Guizhou Uplift (Fig. 13D) and experienced a large marine regression. In addition, the Yangtze Block drifted to low latitudes, resulting in intense weathering and erosion of the Ordovician and Cambrian strata, and the dissolution of carbonate minerals and deposition of insoluble silicate debris in the carbonate rocks of central Guizhou (Fig. 13F). Finally, the clastic material was deposited in nearby karst depressions, experienced physical–chemical–biological weathering, forming the clay of the Jiujialu Formation on top of the Cambrian and Ordovician strata.

The weathered products were exposed to the alkaline environment caused by carbonate weathering that promoted the crystallisation

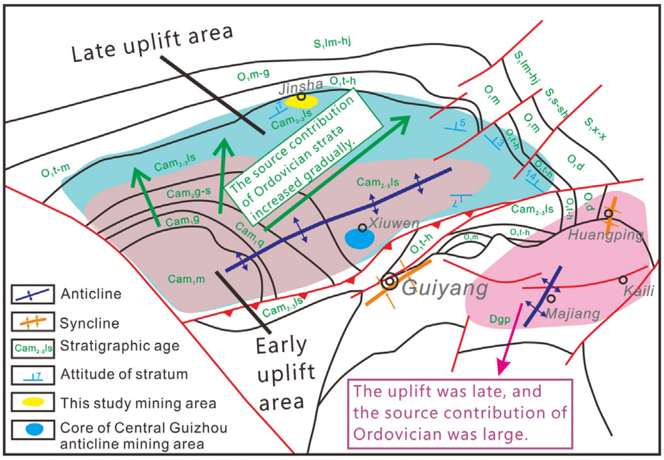

Fig. 10. Detrital contributions of the Loushanguan Group ($Cam_{2-3}ls$) and Ordovician strata to the Li-rich claystone of the Jiujialu Formation (C_1jj).

of smectite and maintained a high cation exchange capacity (Fig. 13E; Wilson, 1999; Gylesjö and Arnold, 2006; Varga et al., 2011; Újvári et al., 2014), leading to the formation of Li-rich claystone. With an increase in weathering intensity, many alkali metal and Si ions were lost; thus, the clay minerals were transformed into boehmite and finally formed bauxite deposits (Öztürk, 2002; Wen et al., 2020).

6. Conclusions

Palaeogeographic, geochemical, and detrital zircon data of the Jiujialu Formation, Loushanguan Group, and Ordovician and Cambrian strata in the South China Block suggest the following sedimentary provenance and place the following constraints on the deposition of the Jiujialu Formation.

1. The Li-rich rocks of the Jiujialu Formation were recycled from sedimentary bedrock. In the core of the Central Guizhou Anticline (i.e., the Xiuwen area), the source material for the Li-rich claystone is the Cambrian carbonate bedrock. Ordovician strata also contributed material to the Jiujialu Formation in the Jinsha area at the margin of the Central Guizhou Uplift, and provided a large contribution to the Jiujialu Formation in the southeastern depression around Huangping, Kaili, and Yudong. Those results suggest that the weathering of sedimentary strata can form clay-type Li deposits in areas with carbonate bedrock.

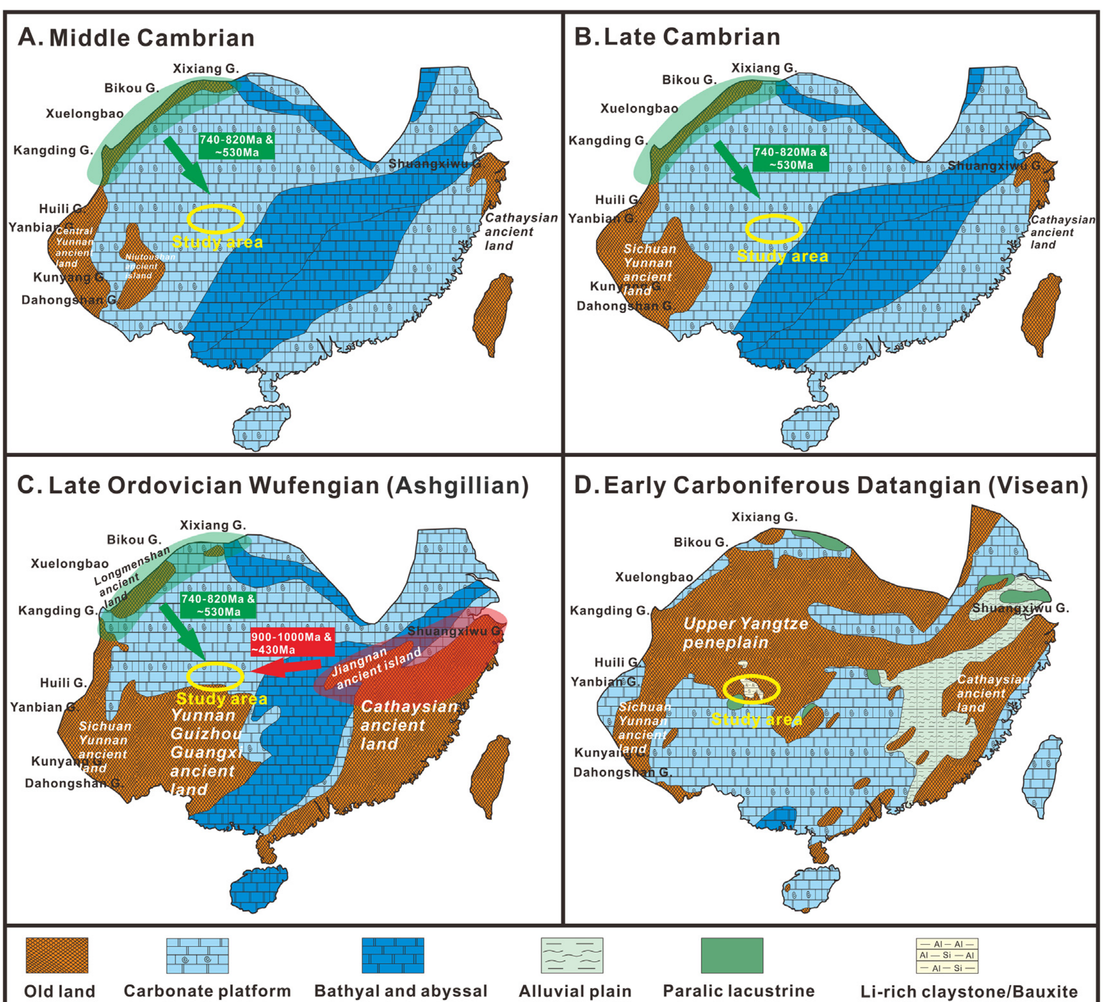

Fig. 11. Transport paths of detrital zircons. The base map is modified from Liu (1994). Arrows indicate the source of the detrital material, and numbers in green and red boxes indicate the ages of detrital zircons. The transparent green and red areas indicate potential provenance areas. (A and B) The northwestern margin of the Yangtze Block provided material to the Cambrian sedimentary strata. (C) The northwestern margin of the Yangtze Block, Jiangnan Island, and the northern part of the Cathaysia landmass provided material to the Ordovician sedimentary strata. (D) Period of diagenesis of the Jiujialu Formation (C_1jj).

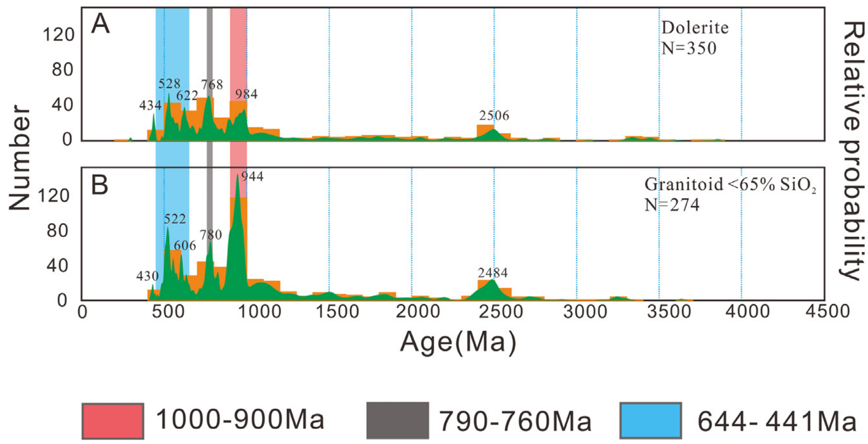

Fig. 12. Probability density plots comparing the U–Pb ages of detrital zircon grains from the Li-rich claystone samples that were derived from (A) dolerite and (B) granitoids with SiO_2 contents of <65 wt%, based on the classification and regression tree analysis (Table 1).

2. The different age peaks of detrital zircons in Li-rich claystone from different regions indicate that the transportation of detritus was limited, and deposition occurred near to the source.
3. The source of material for the Li-rich claystone of the Jiujialu Formation was volcanic rocks of the South China Block, and we propose that mafic rocks at the northwestern margin of the Yangtze Block were the primary provenance of the Jiujialu Formation.
4. The early Palaeozoic intracontinental orogeny in the southeastern part of the South China Block led to uplift of the Cathaysia Block and part of the Jiangnan Orogen Belt, which were then weathered and provided detritus that formed the sedimentary rocks of the Yangtze Block. This may explain the absence of detrital zircon grains with ages of 1000–900 Ma in the Cambrian strata, in contrast to the Ordovician strata.

Supplementary data to this article can be found online at https://doi.org/10.1016/j.sedgeo.2022.106278.

Data availability

No data was used for the research described in the article.

Declaration of competing interest

We declare that we have no financial and personal relationships with other people or organizations that can inappropriately influence our work, there is no professional or other personal interest of any nature or kind in any product, service and/or company that could be construed as influencing the position presented in, or the review of, this manuscript.

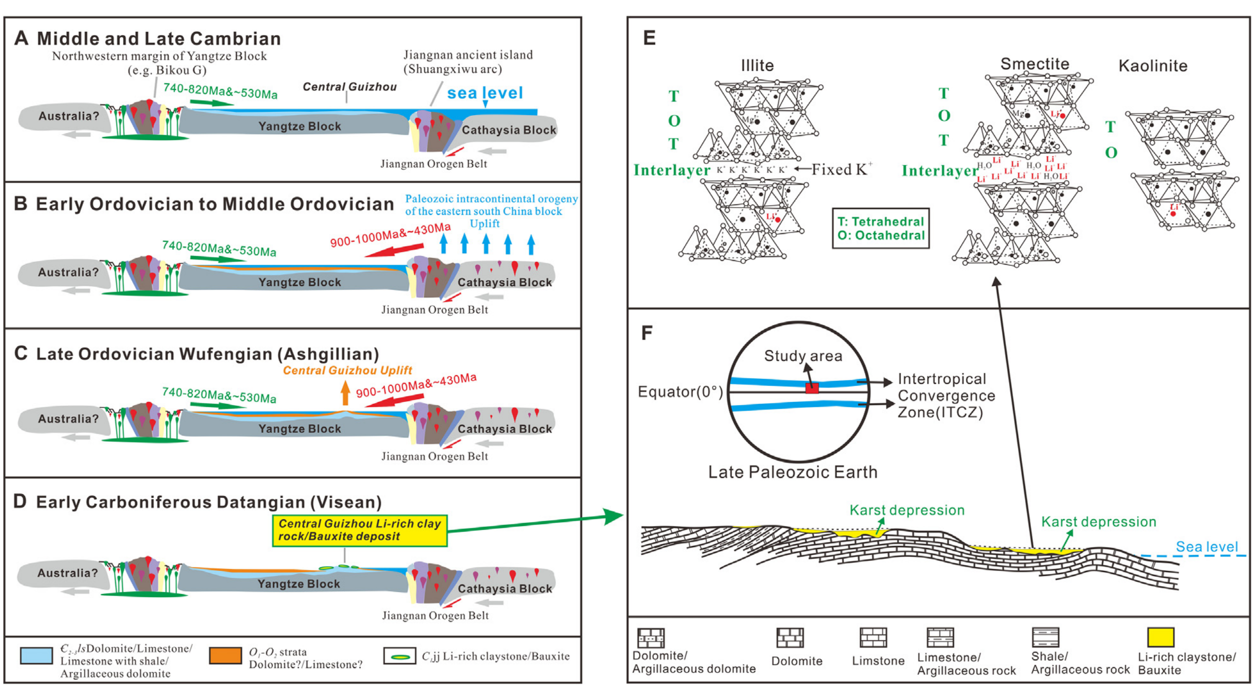

Fig. 13. Simplified model of the formation of Li-rich claystone of the Jiujialu Formation (C_1jj). The smectite structure is modified from Vigier et al. (2008), and the illite and kaolinite structures are modified from Schulze (2005).

Acknowledgments

We thank the Editor in Prof. Brian Jones, reviewer Prof. Paul Karl Link and two anonymous reviewers for their insightful and constructive comments which significantly improved a previous version of the manuscript. We thank A.P. Chuanwei Zhu for his suggestions in writing and Dr. Zhengdong Tian for helping with the graphic works.

This project was financially supported by the National Natural Science Foundation of China (Grant Nos. 92162214, 41773015, U1812402, 42073019, 41903038 and 41962005); Key Research and Development Program of Yunnan Province (202103AQ100003); High precision determination of lead isotopes in environmental samples by MC-ICP-MS (DJNY2021-31).

References

Belousova, E., Griffin, W., O'Reilly, S.Y., Fisher, N., 2002. Igneous zircon: trace element composition as an indicator of source rock type. Contributions to Mineralogy and Petrology 143, 602–622.

Benson, T.R., Coble, M.A., Rytuba, J.J., Mahood, G.A., 2017. Lithium enrichment in intracontinental rhyolite magmas leads to Li deposits in caldera basins. Nature Communications 8, 1–9.

Compston, W., Zhang, Z.C., Cooper, J.A., Ma, G.G., Jenkins, R.J.F., 2008. Further SHRIMP geochronology on the early Cambrian of south China. American Journal of Science 308, 399–420.

Deng, X., Yang, K.G., Liu, Y.L., Xu, Z.B., 2010. Characteristics and tectonic evolution of Qianzhong Uplift. Earth Science Frontiers 17, 79–89 (in Chinese with English abstract).

Faure, M., Shu, L.S., Wang, B., Charvet, J., Monie, P., 2009. Intracontinental subduction: a possible mechanism for the early Palaeozoic Orogen of SE China. Terra Nova 21, 360–368.

Feng, Z.Z., Peng, Y.M., Jin, Z.K., Bao, Z.D., 2004. Lithofacies palaeogeography of the Late Ordovician in China. Journal of Palaeogeography 6, 5–17.

Gao, D.D., Sheng, Z.Q., Shi, S.H., Chen, L.A., 1992. Studies on the Bauxite Deposit in Central Guizhou, China Guiyang. Guizhou Science & Technology Publishing House, Guiyang, pp. 11–20 (in Chinese).

Gao, S., Ling, W.L., Qiu, Y.M., Lian, Z., Hartmann, G., Simon, Klaus, 1999. Contrasting geochemical and Sm–Nd isotopic compositions of Archean metasediments from the Kongling high-grade terrain of the Yangtze craton: evidence for cratonic evolution and redistribution of REE during crustal anatexis. Geochimica et Cosmochimica Acta 63, 2071–2088.

Geng, Y.S., Kuang, H.W., Du, L.L., Liu, Y.Q., 2020. The characteristics of Meso–Neoproterozoic magmatic rocks in North China, South China and Tarim blocks and their significance of geological correlation. Acta Petrologica Sinica 36, 2276–2312 (in Chinese with English abstract).

Gu, J., Huang, Z.L., Fan, H.P., Ye, L., Jin, Z.G., 2013. Provenance of lateritic bauxite deposits in the Wuchuan–Zheng'an–Daozhen area, Northern Guizhou Province, China: LA–ICP–MS and SIMS U–Pb dating of detrital zircons. Journal of Asian Earth Sciences 70–71, 265–282.

Gylesjö, S., Arnold, E., 2006. Clay mineralogy of a red clay–loess sequence from Lingtai, the Chinese Loess Plateau. Global and Planetary Change 51, 181–194.

Han, Z.R., Jing, X.Q., Tong, Y.B., Yang, Z.Y., Sun, H.R., 2017. LA–ICP–MS U–Pb geochronology of detrital zircon from the Lower Ordovician in the Western Yangtze Block and its geological implications. Acta Mineralogica Sinica 37, 218–230 (in Chinese with English abstract).

He, Y.Y., Niu, Z.J., Zhang, Z.Z., Song, F., Yao, H.Z., Yang, W.Q., Gong, Y.J., Wang, Z.W., Gan, J. M., Wang, Z.H., 2020. Detrital zircons of the Meitan Formation during Ordovician in Northeastern Guizhou and its significance for provenance–tectonic and implications for metallogenic chronology. Geology in China 47, 1025–1040 (in Chinese with English abstract).

Hou, Y.L., Zhong, Y.T., Xu, Y.G., He, B., 2017. The provenance of late Permian karstic bauxite deposits in SW China, constrained by the geochemistry of interbedded clastic rocks, and U–Pb–Hf–O isotopes of detrital zircons. Lithos 278–281, 240–254.

Hu, Z.R., Zhang, X.L., Liu, X.F., 1988. The carboniferous Jiujialu Formation (C_1jj) and its environments. Geology of Guizhou 2, 135–142 (in Chinese with English abstract).

Hu, Z.C., Zhang, W., Liu, Y.S., Gao, S., Li, M., Zong, K.Q., Chen, H.H., Hu, S.H., 2015. "Wave" signal-smoothing and mercury-removing device for laser ablation quadrupole and multiple collector ICPMS analysis: application to lead isotope analysis. Analytical Chemistry 87, 1152–1157.

Kesler, S.E., Gruber, P.W., Medina, P.A., Keoleian, G.A., Everson, M.P., Wallington, T.J., 2012. Global lithium resources: relative importance of pegmatite, brine and other deposits. Ore Geology Reviews 48, 55–69.

Kong, H., Wu, J.H., Li, H., Chen, S.F., Liu, B., Wang, G., 2020. Early Paleozoic tectonic evolution of the South China Block: constraints from geochemistry and geochronology of granitoids in Hunan Province. Lithos 380–381, 105891. https://doi.org/10.1016/j.lithos.2020.105891.

Li, X.H., Zhou, H.W., Li, Z.X., Liu, Y., 2001. Zircon U–Pb age and petrochemical characteristics of the Neoproterozoic bimodal volcanics from western Yangtze block. Geochimica 30, 315–322 (in Chinese with English abstract).

Li, X.H., Li, Z.X., Zhou, H.W., Liu, Y., Kinny, P.D., 2002. U–Pb zircon geochronology, geochemistry and Nd isotopic study of Neoproterozoic bimodal volcanic rocks in the Kangdian Rift of South China: implications for the initial rifting of Rodinia. Precambrian Research 113, 135–154.

Li, X.H., Wang, X.C., Li, W.X., Li, Z.X., 2008a. Petrogenesis and tectonic significance of Neoproterozoic basaltic rocks in South China: from orogenesis to intracontinental rifting. Geochimica 37, 382–398 (in Chinese with English abstract).

Li, X.H., Li, W .X., Li, Z.X., Liu, Y., 2008b. 850~890 Ma bimodal volcanicand intrusive rocks in northern Zhejiang, South China: a major episode of continental rift magmatism during the breakup of Rodinia. Lithos 102, 341–357.

Li, X.H., Li, W.X., Li, Z.X., Lo, C.H., Wang, J., Ye, M.Y., Yang, Y.H., 2009. Amalgamation between the Yangtze and Cathaysia Blocks in South China: constraints from SHRIMP U–Pb zircon ages, geochemistry and Nd–Hf isotopes of the Shuangxiwu volcanic rocks. Precambrian Research 174, 117–128.

Ling, K.Y., Tang, H.S., Zhang, Z.W., Wen, H.J., 2020. Host minerals of Li–Ga–V–rare earth elements in Carboniferous karstic bauxites in southwest China. Ore Geology Reviews 119, 103325. https://doi.org/10.1016/j.oregeorev.2020.103325.

Liu, B., 1994. Atlas of the Lithofacies and Palaeogeography of South China (Sinian-Triassic). Paleogeography.

Liu, B.J., Xu, X.S., 1994. Atlas of the Lithofacies and Palaeogeography of South China (Sinian-Triassic). Science Press, Beijing, pp. 72–136 (in Chinese).

Liu, Y.S., Hu, Z.C., Gao, S., Günther, D., Xu, J., Gao, C.G., Chen, H.H., 2008. In-situ analysis of major and trace elements of anhydrous minerals by LA–ICP–MS without applying an internal standard. Chemical Geology 257, 34–43.

Liu, Y.S., Gao, S., Hu, Z.C., Gao, C.G., Zong, K.Q., Wang, D.B., 2010. Continental and oceanic crust recycling-induced melt–peridotite interactions in the Trans–North China Orogen: U–Pb dating, Hf isotopes and trace elements in zircons of mantle xenoliths. Journal of Petrology 51, 537–571.

Ludwig, K.R., 2003. ISOPLOT 3.00: A Geochronological Toolkit for Microsoft Excel. Berkeley Geochronology Center, California, Berkeley (39 pp.).

Mojzsis, S.J., Harrison, T.M., Pidgeon, R.T., 2001. Oxygen–isotope evidence from ancient zircons for liquid water at the Earth's surface 4, 300 Myr ago. Nature 409, 178–181.

Nemchin, A.A., Pidgeon, R.T., Whitehouse, M.J., 2006. Re-evaluation of the origin and evolution of >4.2 Ga zircons from the Jack Hills metasedimentary rocks. Earth and Planetary Science Letters 244, 218–233.

Niu, X.S., Feng, C.M., Liu, J., 2007. Formation mechanism and time of Qianzhong (Central Guizhou) uplift. Marine Origin Petroleum Geology 12, 46–50 (in Chinese with English abstract).

Öztürk, Hüseyin., 2002. Genesis of the Doğankuzu and Mortaş Bauxite Deposits, Taurides, Turkey: separation of Al, Fe, and Mn and implications for passive margin metallogeny. Economic Geology 97, 1063–1077.

Paul, W.G., Pablo, A.M., Gregory, A.K., Stephen, E.K., Mark, P.E., Timothy, J.W., 2011. Global lithium availability. Journal of Industrial Ecology 15, 760–775.

Qiu, Y.M., Gao, S., Mcnaughton, N.J., Groves, D.I., Ling, W.L., 2000. First evidence of >3.2 Ga continental crust in the Yangtze craton of south China and its implications for Archean crustal evolution and Phanerozoic tectonics. Geology 28, 11–14.

Schulze, D.G., 2005. Clay minerals. Encyclopedia of Soils in the Environment 246–254.

Shu, L.S., 2012. An analysis of principal features of tectonic evolution in South China Block. Geological Bulletin of China 31, 1035–1053 (in Chinese with English abstract).

Siebel, W., Schmitt, A.K., Danišík, M., Chen, F.k., Meier, S., Weiß, S., Eroğlu, S., 2009. Prolonged mantle residence of zircon xenocrysts from the western Eger rift. Nature Geoscience 2, 886–890.

Tarascon, J.M., 2010. Is lithium the new gold? Nature Chemistry 2, 510.

Újvári, G., Varga, A., Raucsik, B., Kovács, J., 2014. The Paks loess–paleosol sequence: a record of chemical weathering and provenance for the last 800 ka in the mid-Carpathian Basin. Quaternary International 319, 22–37.

Varga, A., Újvári, G., Raucsik, B., 2011. Tectonic versus climatic control on the evolution of a loess–paleosol sequence at Beremend, Hungary: an integrated approach based on paleoecological, clay mineralogical, and geochemical data. Quaternary International 240, 71–86.

Vigier, N., Decarreau, A., Millot, R., Carignan, J., Petit, S., France-Lanord, C., 2008. Quantifying Li isotope fractionation during smectite formation and implications for the Li cycle. Geochimica et Cosmochimica Acta 72, 780–792.

Wang, X.L., Shu, L.S., Xing, G.F., Zhou, J.C., Tang, M., Shu, X.J., Qi, L., Hu, Y.H., 2012a. Post–orogenic extension in the eastern part of the Jiangnan Orogen: evidence from ca. 800~760Ma volcavic rocks. Precambrian Research 222–223, 404–423.

Wang, L.J., Yu, J.H., Griffin, W.L., O'Reolly, S.Y., 2012b. Early crustal evolution in the western Yangtze Block: evidence from U–Pb and Lu–Hf isotopes on detrital zircons from sedimentary rocks. Precambrian Research 222–223, 368–385.

Wang, L.J., Griffin, W.L., Yu, J.H., O'Reolly, S.Y., 2013. U–Pb and Lu–Hf isotopes in detrital zircon from Neoproterozoic sedimentary rocks in the northern Yangtze Block: implications for Precambrian crustal evolution. Gondwana Research 23, 1261–1272.

Wang, R.X., Wang, Q.F., Huang, Y.X., Yang, S.J., Liu, X.F., Zhou, Q., 2018. Combined tectonic and paleogeographic controls on the genesis of bauxite in the Early Carboniferous to Permian Central Yangtze Island. Ore Geology Reviews 101, 468–480.

Wen, Z., 2013. Study on Lithofacies Palaeogeography of the Middle and Late Cambrian in the Middle and Upper Yangtze Region. Yangtze University, Jingzhou, Hubei Province, pp. 83–84.

Wen, H.J., Luo, C.G., Du, S.J., Yu, W.X., Gu, H.N., Ling, K.Y., Cui, Y., Li, Y., Yang, J.H., 2020. Carbonate-hosted clay-type lithium deposit and its prospecting significance. Chinese Science Bulletin 65, 53–59 (in Chinese with English abstract).

Wilson, M.J., 1999. The origin and formation of clay minerals in soils past present and future perspectives. Clay Minerals 34, 7–25.

Xiong, G.L., Yu, W.C., Du, Y.S., Weng, S.F., Pang, D.W., Deng, X.S., Zhou., J.T., 2021. Provenance of lower carboniferous bauxite deposits in Northern Guizhou, China: constraints from geochemistry and detrital zircon U–Pb ages. Journal of Earth Science 32, 235–252.

Xu, Y.J., Du, Y.S., 2018. From periphery collision to intraplate orogeny: Early Paleozoic orogenesis in southeastern part of south China. Earth Science 43, 333–353.

Yu, W.C., Thomas, J.A., Yan, J.X., Yang, J.H., Du, Y.S., Huang, X., Weng, S.F., 2019. Climatic and hydrologic controls on upper Paleozoic bauxite deposits in South China. Earth-Science Reviews 189, 159–176.

Zhang, F.F., Wang, Y.J., Zhang, A.M., Fan, W.M., Zhang, Y.Z., Zi, J.W., 2012. Geochronological and geochemical constraints on the petrogenesis of Middle Paleozoic (Kwangsian) massive granites in the eastern South China Block. Lithos 150, 188–208.

Zhang, C., Li, Z.L., Chen, Q.J., Dong, S.P., Yu, X.H., Yu, Q.J., 2020. Provenance of eolian sands in the Ulan Buh Desert, northwestern China, revealed by heavy mineral assemblages. CATENA 193, 104624. https://doi.org/10.1016/j.catena.2020.104624.

Zhang, S.W., Wang, F., Xu, W.L., Gao, F.H., Tang, J., 2021. Tectonic history of the Huangsong tectonic terrains in the Khanka Massif in the easternmost Central Asian Orogenic Belt: constraints from detrital zircon U–Pb geochronology. Gondwana Research 99, 149–162.

Zhao, G.C., Cawood, P.A., 1999. Tectonothermal evolution of the Mayuan assemblage in the Cathaysia Block: implications for Neoproterozoic collision-related assembly of the south China craton. American Journal of Science 288, 309–339.

Zhao, L.H., Liu, X.F., 2019. Metallogenic and tectonic implications of detrital zircon U–Pb, Hf isotopes, and detrital rutile geochemistry of late carboniferous karstic bauxite on the southern margin of the North China Craton. Lithos 350–351, 105222. https://doi.org/10.1016/j.lithos.2019.105222.

Zheng, Y.F., Zhang, S.B., 2007. Formation and evolution of Precambrian continental crust in South China. Chinese Science Bulletin 52, 1–10 (in Chinese).

Zheng, J.P., Griffin, W.L., O'Reilly, S.Y., Zhang, M., Pearson., N., Pan, Y.P., 2006. Widespread Archean basement beneath the Yangtze craton. Geology 34, 417–420.

Zhu, R.X., Li, X.H., Hou, X.G., Pan, Y.X., Wang, F., Deng, C.L., He, H.Y., 2009. SIMS U–Pb zircon age of a tuff layer in the Meishucun section, Yunnan, southwest China: constraint on the age of the Precambrian–Cambrian boundary. Science in China, Series D: Earth Sciences 39, 1105–1111 (in Chinese without English abstract).

Zhu, X.Y., Wang, B., Sun, Z.C., Liu, J.S., He, Z.Y., Zhong, L.L., 2020. Detrital zircon ages of the Mesoproterozoic metasedimentary rocks in the southern Yili Block: implications for tectonic affinities of the microcontinents in SW Central Asian Orogenic Belt. Precambrian Research 350, 105926. https://doi.org/10.1016/j.precamres.2020.105926.

Zong, K.Q., Klemd, R., Yuan, Y., He, Z.Y., Guo, J.L., Shi, X.L., Liu, Y.S., Hu, Z.C., Zhang, Z.M., 2017. The assembly of Rodinia: the correlation of early Neoproterozoic (ca. 900 Ma) high–grade metamorphism and continental arc formation in the southern Beishan Orogen, southern Central Asian Orogenic Belt (CAOB). Precambrian Research 290, 32–48.